Deduction of Radon Diffusion Process from Natural Radioactive Porous Samples Collected from Sinai-Egypt

Hanan A. S. Aly

Physics Department, Faculty of Women for Arts, Science and Education, Ain Shams University, Cairo, Egypt.

ABSTRACT

This work develops a straightforward investigation method for estimating the behaviour of radon diffusion from natural radioactive sample content a radium activity to sample surfaces. In the current inquiry, a dual approach is adopted. First, the HPGe detector was used to measure the radium activity concentration, and the radon activity corresponding to the measured radium content was computed. Second, the (SSNTD) CR-39 accumulation chamber was used to record the radon activity emanating from natural materials. Finally, a comparison of the results from the two approaches demonstrates that leakage and diffusion processes cause the real radon in any sample to be more than the radon that has been detected. The impact of sample layer thickness on radon detection has been studied, and the findings indicate that maximum radon measurement is more effectively accomplished at layer thicknesses of 50 mm.

Keywords: Radon, HPGe, SSNTD CR-39, Radon diffusion, Radium content.

1. Introduction

Due to its short half-life (3.8 days) and extended diffusion time through the surface, radon can significantly degrade in the cover Radon is produced over thousands of years at roughly steady rates in uranium mill tailings. As a result, forecasting radon flows or concentrations as well as the impact of different materials are crucial for constructing the necessary covers. Additionally, measurements of radon emissions from residue repositories can be used as experimental input for mathematical models of radon emission to the atmosphere (Rogers and Nielson, 1991).

The ratio of released radon atoms to created radon atoms is known as the radon emission fraction. Different minerals have different radon emanation fractions, which are improved by rising temperatures, moisture levels, and specific surface areas (Sakoda *et al.,* 2010).

An internal danger is brought on by -particles that enter the body when radon and its offspring are inhaled, as opposed to an exterior hazard, which results from direct contact with -ray radiation. Despite having a brief lifespan, these substances accumulate on the tissues of the respiratory tract (UNSCEAR, 1993), Even for the same type of material, there can be some variations in radon diffusion coefficient values because the radon diffusion coefficient depends on the chemical composition of the material as well as manufacturing, material density, raw materials, concentration gradient on both sides of the barrier (Szajerski and Zimny, 2020). this demonstrates the significance of testing natural sedimentary rocks for radon activity concentrations, which are consider as a main raw materials used in a variety of industries.

According to the World Health Statistics 2018, one of the linked sustainable development goals for urban development of cities should be to ensure healthy lifestyles and promote well-being for all ages (WHO, 2018). Additionally, rocks are the primary location where natural radon gas is stored (Huang *et al.,* 2021).

Corresponding Author: Hanan. A. S. Aly, Physics Department, Faculty of Women for Arts, Science and Education, Ain Shams University, Cairo, Egypt.
E-mail: hanan_ali2@women.asu.edu.eg

Rocks' radon exhalation properties have been employed by numerous nations in recent years to forecast rock destabilisation and conduct environmental assessments in a variety of industries (Pepperosa *et al.,* 2022 & Silva and Dinis, 2022).

The creation of various decay products of radioactive series, such as radon and its progeny, is a key cause for concern with regard to Naturally Occurring Radioactive Material (NORM) (Abu-Haija, 2012). The principal determinants of the rate of radon precipitation in rock and soil are porosity, specific surface area, and radon diffusion coefficient, pore water filling level, temperature, radium concentration, and radium -226 content (Abd Ali *et al.,* 2019).

To establish reliable radon activity concentration rates in relation to the radium content responsible for this activity, more research is required. In order to analyse the relationship between radon activity and radium content as well as anticipate radon activity that would be consistent with naturally occurring radium activity, this study compared the two.

Using a P type High purity germanium detector (HPGe), gamma spectra have been accumulated and analysed to measure radium and radon progeny activity have been measured. Also the amount of radon in the air was measured using the Solid State Nuclear Track Detector (SSNTD).

2. Methodology
2.1. Sample characteristics

Eight samples were chosen from Egypt's north-western Sinai, at Um Bogma formation, the chosen study region, is significant because it provides a significant amount of the raw minerals needed by many purposes. The upper Earth is thought to be the stratigraphic region of the crust where uranium-bearing sediments are mostly constrained and connected to these formation sediments (Yan *et al.,* 2019), Table 1: shows studied samples features.

Table 1: Descriptions of samples.

S1	Dark brown to grey, silty shale highly ferruginous
S2	Dark grey to black shale with patches of gypsum
S3	Sandydolostone, dark grey gypsum.
S4	Dark brown, soft, highly ferruginous
S5	Black sediment, soft to weakly cemented
S6	Dark black, soft sediment
S7	Dark brown to black sediment
S8	Black powdery sediments

2.2. Sample Preparation

Using a random sampling technique, eight sedimentary rock samples were collected from the studied area. After that, the samples were packaged, labelled, and brought to the lab. In order to attain secular equilibrium and prevent the escape of ^{222}Rn and ^{220}Rn, each sample was physically crushed, air-dried in a dry environment, and sieved through a 2 mm mesh sieve before being sealed in 100 ml polyethylene Marinelli beakers (Nada and Aly, 2014).

2.3. Experimental Technique.
A. HPGE Detector.

Using an HPGe detector, the samples were non-destructively analyzed. Because of their superior energy resolution and the fact that they are a non-destructive method that doesn't require any chemical preparation or radionuclide separation, hyper pure germanium (HP-Ge) gamma ray spectrometry instruments are commonly employed for radioactivity analysis (Knoll, 2000). The radiometric measurements were carried out using a vertically positioned, liquid nitrogen-cooled, closed-end coaxial gamma-ray detector (p-type), manufactured of high purity germanium (HPGe). The full width at half maximum (FWHM) of the employed HPGe EG&G Ortec Model. The system exhibits a peak/Compton ratio of 56:1 at the 1.33 MeV gamma transition of 60Co, a resolution of 2.3 keV, and a relative efficiency of roughly 60% of the 300 300 NaI (Tl) crystal efficiency. The energy of the device was calibrated to show gamma photo peaks between 63 and 3000 keV. Three well-known reference materials received from the International Atomic Energy Agency for measurements of U, Th, and K activity were used for the efficiency calibration: RGU-1, RGTh-1, and RGK-1 (Anjos *et al.,* 2005). Gamma spectrum peak

area analysis is performed using Genie 2000 software and a period of 80,000s that is customised for each sample. The specific activity of ^{226}Ra was measured using the 186.1 keV peak from its own gamma-ray emission (after the subtraction of the 185.7 keV peak of ^{235}U). The specific activity of ^{214}Pb was measured using the 295.2 keV and 351.9 keV peaks, whereas the specific activity of ^{214}Bi was measured using the 609.3 keV peak.

In the current study, the specific activity (C) in units of BqKg^{-1} is calculated using the equation below. (Anjos *et al.,* 2005):

$$C = \frac{C_n}{\varepsilon P_\gamma M_S} \quad (1)$$

Where
C_n is the count rate under each photo-peak due to each radionuclide,
ε is the detector efficiency for the specific γ-ray,
P_γ is the intensity of the specific γ-ray, and
M_S is the mass of the sample which is measured in kg in our study.

B. Radon measurements

Solid state nuclear track detectors can pick up on alpha particles with an energy range comparable to the radon particles (SSNTD) (Mansy *et al.,* 2006). The detectors were (CR-39) with a 1 cm2 surface area and a 1 mm thickness. The detectors were set up and placed at the bottom of the chamber cover, as shown in Fig. 1. 30 days after the chamber was sealed, the samples were retained. During this exposure period, radon and its daughters' alpha particles entered the air volume of the chamber and were detected by the CR-39. The chamber cover was taken off, and the detectors were chemically etched in a 6.25 N solution of NaOH for six hours at 70°C.
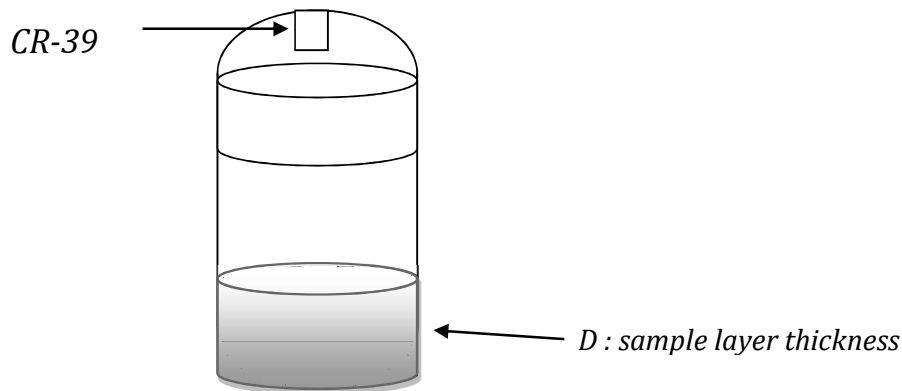

Fig. 1: CR-39 Set up in Chamber Cover

By examining photos captured by a 400x optical microscope, the engraved traces on the detectors were manually numbered. The area of one field of view was measured using a stage eyepiece, and the track density was calculated in tracks per cm2. The background track density was determined by etching a brand-new detector under the same circumstances. The measured track density was reduced by the background.

Two ways for radon to migrate through porous material are diffusive and adjective transit. Given that there is no radon production and that the test specimen solely experiences pure diffusive radon transport.

To get accurate statistics of the tracks, twenty fields of view on the detector surface were randomly selected. According to the following equation.2 provided by Khan *et al.* (1990), the calibration factor of 0.18 + 0.002 tracks cm², obtained from a prior track detector calibration experiment (CR-39) (Miroslaw *et al.,* 2021), was used to calculate the radon activity from the track density as follow:

$$C_{Rn} = \frac{(N - B)}{t\, C_F} \quad (2)$$

where C_{Rn} is the mean ^{222}Rn concentration in Bqm^{-3}, N is the track density (Track.cm^{-2}), B is the background track density (Track.cm^{-2}), C_F is the calibration factor in cm^{-2} d^{-1} per Bqm^{-3}, and t is the exposure duration (in hours).

3. Results and Discussions
3.1 Activity concentrations

Based on reordered gamma spectra, Table.2 shows the activities concentration of ^{226}Ra and radon progeny, ^{214}Bi and ^{214}Pb, for various samples. Fig.2 display activity concentration for radium and radon progeny for different samples.

Table 2: ^{226}Ra ^{214} Bi and ^{214}Pb activity concentrations for different samples

Sample	^{226}Ra	^{214}Pb	^{214}Bi
S1	5033.39 ± 81.59	6656.67± 61.59	7450.69 ± 68.24
S2	7091.13 ± 76.34	8300.25 ± 65.52	6307.49 ± 92.38
S3	9414.52 ± 51.89	11036.22 ± 42.29	11309.30 ± 116.09
S4	10946.62 ± 211.67	11756.99 ± 101.24	12896.31± 86.34
S5	5468.33 ± 67.09	5757.09 ± 56.42	6592.15 ± 90.41
S6	4540.99 ± 101.34	5234.90 ± 95.16	5469.13 ± 75.22
S7	6422.24 ± 78.49	7859.96 ± 81.69	8978.97 ± 80.09
S8	7551.41 ± 104.95	7916.78 ± 54.92	8808.74 ± 36.31

Also computed radon concentrations from the CR-39 recorded tracks using equation.2, and the results were compared with the expected radon emission based on the radium activity measured by gamma counting of several examined samples as reported, as listed in Table.3, Fig.3 display radon distribution for different samples.
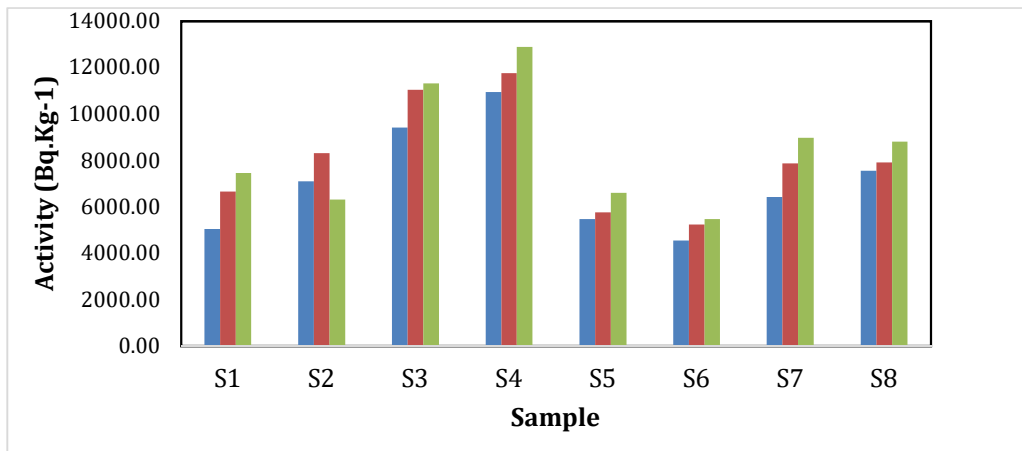

Fig. 2: Activity distribution of radium and radon progeny for different samples

Table 3: Experimental and Calculated of Radon Concentration (atom cm^{-3}).

Sample	^{222}RnC expatom. Cm-3	Mass	P	^{226}Ra Bq=^{222}Rn (atom. Cm^{-3}) (ATSDR, 2012) [18]	Loss%
S1	329.40	214.68	1.07	1080.57	69.52
S2	363.42	241.95	1.21	1715.71	78.82
S3	402.59	247.24	1.24	2327.65	82.70
S4	431.08	248.98	1.24	2725.45	84.18
S5	453.89	192.82	0.96	1054.38	56.95
S6	430.58	179.52	0.90	815.20	47.18
S7	371.20	221.22	1.11	1420.75	73.87
S8	402.05	230.95	1.15	1744.01	76.95

The loss in recorded radon, calculated from the measured radon and Ra activities, explains the ratio of the recorded radon from the true radon observed due to 226Ra decay has been found proportional to sample density.
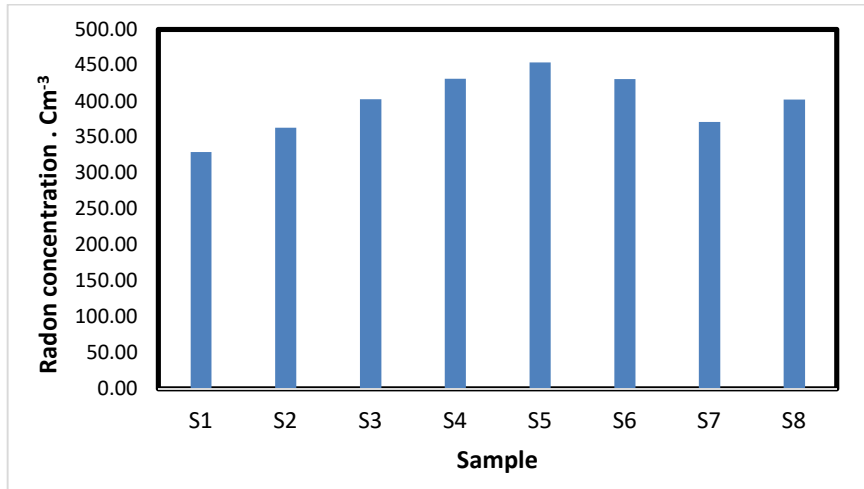

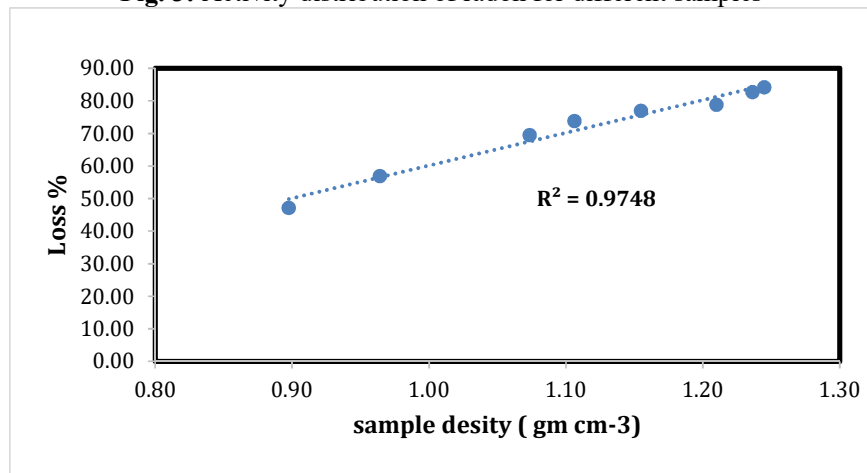**Fig. 3:** Activity distribution of radon for different samples

Fig. 4: Correlation between Loss percent of Radon and sample density

3.2 Effect of sample layer on recorded radon

Sample layer thickness effect on recorded radon from the accumulated radon within chamber has been accomplished for several samples at the same above conditions for radon measurements. Results for different studied eight samples with sample layer ranges of 30-100 mm have been listed in Table 4.

Table. 4: Radon concentrations.cm^{-3} recorded for studied samples and different x.

X (mm)	S1	S2	S3	S4	S5	S6	S7	S8
30	124.5	134.5	185.3	200.6	214.8	198.9	164.5	185.5
40	216.4	233.1	289.4	303.5	305.7	287.5	256.4	289.6
50	329.4	363.4	402.6	431.1	453.9	430.6	371.2	401.1
60	299.6	301.3	342.1	365.9	401.2	372.4	339.6	342.3
70	224.7	245.9	302.9	314.3	364.2	304.5	264.7	303.1
80	201.3	210.13	266.5	287.5	309.6	268.9	241.3	266.7
90	152.6	176.2	202.9	224.7	276.4	219.3	192.2	203.1
100	138.7	145.4	189.2	198.7	226.1	201.6	178.8	189.4

Results from Table.4 have been shown in Fig. 5. It has been demonstrated that adding thin layers of sample causes the amount of recorded Rn to increase until X = 50 mm, after which the quantity of

recorded Rn decreases as sample thickness increases beyond 50 mm. This was anticipated as a result of the back diffusion of radon molecules, which in agreement with Amin, *et al.,* (2018) and Amin, (2015).

Radon atoms stored within solid grains are unlikely to become available for emission to the environment due to their incredibly low diffusion coefficients in materials. However, if they are discovered in the spaces between the grains, they might rise to the top. Consequently, the following series of processes are what lead to radon emissions into the environment from a residue repository (Azeez *et al.,* 2021).
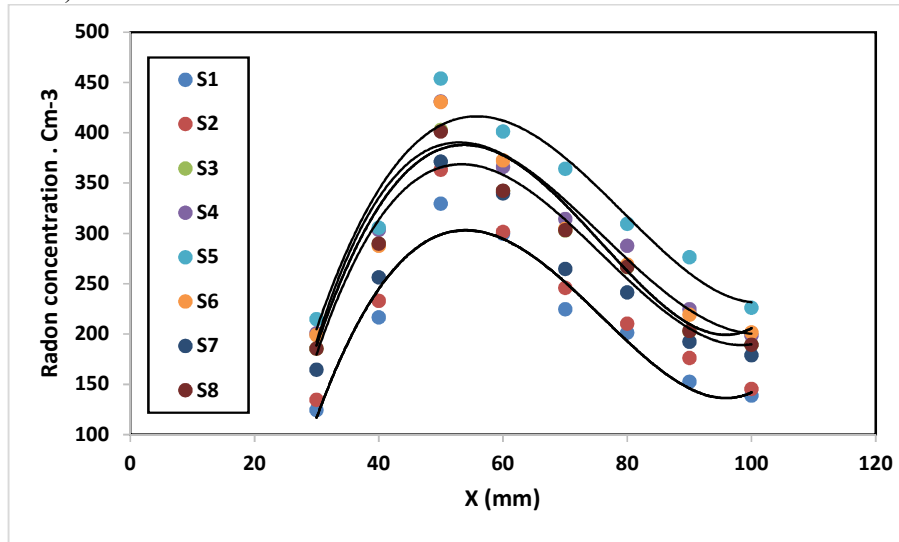

Fig. 5: Radon concentration vs sample layer thickness for different samples

4. Conclusions

The goal of the current investigation was to determine the concentration of radon, radium's mobile daughter gas, in the Um-Bogma area. Gamma counting and SSNTD techniques were used to measure radon concentration and activity in order to study radon diffusion. Results reveal that sample density and layer substantially influenced true radon activity, which corresponds to radium activity that was lost and not reported. The average activity concentration of radionuclides in different samples was displayed. . A good correlation, $R^2=0.98$, has been discovered between the loss of radon present and sample density. This describes the impact of sample structure on radium distribution on grain surface.

Declarations
Conflict of interest: There are no material financial or non-financial interests to disclose for the author.
Ethical approval: There are no studies by any of the writers in this article that used humans or animals as subjects.

References
Abd Ali, F.S., K.H. Mahdi, and E.A. Jawad, 2019: Humidity effect on diffusion and length coefficient of radon in soil and building materials, Energy Procedia, 157: 384.
Abu-Haija, O., 2012. Determination of natural radionuclides concentrations in surface soil in Tafila/Jordan, Modern Appl. Sci., 6: 87.

Amin, S.A., M.A. Al-Khateeb, and T.A. Al Shammar, 2018. Assessment of radon concentrations in the soil of south Baghdad suburbs Ibn Al-Haitham J. For Pure & Appl. Sci., 31:60.

Amin, R.M., 2015. A study of radon emitted from building materials using solid state nuclear track detectors Radiation Research and Applied Science, 8: 516.

Anjos, R.M., R. Veiga, T. Soares, A.M.A. Santos, J.G. Aguiar, M.H.B.O. Frasca, *et al.,* 2005. Natural radionuclide distribution in Brazilian commercial granites. Radiation Measurements, 39:245.

ATSDR, Agency for Toxic Substances and Disease Registry, 2012. Toxicological profile for radon, Public Health Service Agency for Toxic Substances and Disease Registry, Atlanta, Georgia.

Azeez, H.H., M.A. Mohammed, and G.M. Abdullah, 2021. Measurement of radon concentrations in rock samples from the Iraqi Kurdistan region using passive and active methods, Arabian Journal of Geosciences, 13:7.

Huang, Z., W. Zeng, Q. Gu, Y. Wu, W. Zhong, and K. Zhao, 2021. Investigations of variations in physical and mechanical properties of granite, sandstone, and marble after temperature and acid solution treatments Constr. Build. Mater. b: 307.

Khan, A.J., A.K. Varshney, R. Parsed, R.K. Tyagi, and T.V. Ramachandran, 1990. "Calibration of (CR-39) plastic track detector for the measurement of radon and its daughters in dwellings". Nucl Tracks Radiat Measure, 17: 497.

Knoll, G.F., 2000. Radiation Detection and Measurement, 3rd dition. New York, USA: John Wiley and Sons Inc.

Mansy, M., M.A. Sharaf, H.M. Eissa, S.U. El-Kamees and M. Abo-Elmagd, 2006. Theoretical calculation of SSNTD response for radon measurements and optimum diffusion chambers dimensions, Radiation Measurements, 14:222.

Miroslaw, J., H. Mahamudul, B. Peter, and K. Norbert, 2021: Effects of Storage Time and Pre-Etching Treatment of CR-39 Detectors on Their Response to Alpha Radiation Exposure, Int. J. Environ. Res. Public Health, 19: 8346.

Nada, A. and H.A.S. Aly, 2014. The effect of uranium migration on radionuclide distributions for soil samples at the El-Gor area, Sinai, Egypt, Applied Radiation and Isotopes, 84:79.

Pepperosa, A., R. Remetti, and F. Perondi, 2022. ARMAX forecast model for estimating the annual radon activity concentration in confined environment by short measurements performed by active detectors Int. J. Environ. Res. Public Health, 19: 5229.

Rogers, V., and K. Nielson, 1991. Correlations for predicting air permeabilities and Rn diffusion coefficients of soils. Health Phys., 61: 225.

Sakoda, A., Y. Nishiyama, K. Hanamoto, Y. Ishimori, Y. Yamamoto, T. Kataoka, A. Kawabe, and K. Yamaoka, 2010. Differences of natural radioactivity and radon emanation fraction among constituent minerals of rock or soil. Appl. Radiat. Isot., 68:1180.

Silva, A.S., and M.D.L. Dinis, 2022. Assessment of indoor radon concentration and time-series analysis of gamma dose rate in three thermal spas from Portugal, Environ. Monit. Assess., 194: 1.

Szajerski, P., and A. Zimny, 2020. Numerical analysis and modeling of two-loop experimental setup for measurements of radon diffusion rate through building and insulation materials Environ. Pollut., 256: 113393.

UNSCEAR., 1993. United Nations Scientific Committee on the Effect of Atomic Radiation. Sources and Effects of Ionizing Radiation; UNSCEAR, New York, NY, USA.

WHO, World health statistics 2018. Monitoring health for the SDGs – Sustainable development goals, World Health Organization, Geneva.

Yan, B., X. Zhu, X. He, and S. Tang, 2019: Zn Isotopic evolution in early Ediacaran ocean: a global signature Precambr. Res., 320: 472.